Can. J. Remote Sensing, Vol. 33, No. 6, pp. 468–480, 2007

Cerrado vegetation study using optical and radar remote sensing: two Brazilian case studies

Marisa D. Bitencourt, Humberto N. de Mesquita, Jr., Gerardo Kuntschik, Humberto R. da Rocha, and Peter A. Furley

Abstract. The amount of phytomass is a crucial parameter in ecology as a whole. Conventional methods to estimate phytomass parameters are often prohibitive in terms of time, environment, and manpower. Seasonality in Brazilian savanna physiognomies is marked by green leaves lost during the dry season and regrowth during the wet season. Branches and trunks remain the same through the seasons. The amounts of the phytomass components can be estimated by nondestructive methods using remote sensing. This paper presents case studies where the abilities to predict vegetation variation are tested using optical and radar images. The foliar component leaf area index (LAI) obtained in the field is related to the normalized difference vegetation index (NDVI) obtained from satellite images, and both methods present a strong relationship with green leaves biomass. Japanese Earth Resources Satellite (JERS-1) images are used to estimate the aboveground woody biomass. *Campo cerrado* physiognomy showed the highest seasonal variation in NDVI, and *cerradão* the lowest variation in NDVI. During August, the lower the NDVI values, the lower the solar albedo and the higher the photosynthetically active radiation (PAR) albedo. During November, the higher the NDVI values, the lower the PAR and the higher the solar albedo. The same proportion in seasonal variation was observed with LAI values. A significant equation is proposed to estimate trunk and branch biomass using allometric parameters and JERS-1 backscattering.

Résumé. La quantité de phytomasse est un paramètre crucial pour l'écologie en général. Les méthodes conventionnelles pour l'estimation des paramètres de la phytomasse sont souvent prohibitives en termes de temps, d'environnement et de main-d'œuvre. La saisonnalité dans les physionomies de savane au Brésil est marquée par la perte des feuilles vertes durant la période sèche et la repousse durant la saison humide. Les branches et les troncs demeurent inchangés à travers les saisons. La quantité de composantes de la phytomasse peut être estimée à l'aide de méthodes non destructives en utilisant la télédétection. Cet article présente des exemples où les capacités de prévision des variations dans la végétation sont testées à l'aide d'images optiques ou radar. La composante foliaire LAI (« leaf area index »), obtenue sur le terrain, est reliée au NDVI (« normalized difference vegetation index ») dérivé d'images satellitaires, et les deux méthodes montrent des relations fortes avec la biomasse des feuilles vertes. Des images JERS-1 (« Japanese Earth Resources Satellite ») sont utilisées pour estimer la biomasse ligneuse aérienne. La physionomie de type *campo cerrado* (savane arbustive) a affiché la plus grande variation au niveau du NDVI alors que la physionomie de type *cerradão* (savanne arborée) a montré la variation la plus faible du NDVI au cours des saisons. Au cours du mois d'août, plus les valeurs du NDVI sont faibles, plus l'albédo solaire est faible et plus l'albédo PAR (« photosynthetically active radiation ») est élevé. Au cours du mois de novembre, plus les valeurs du NDVI sont élevées, plus les valeurs de PAR sont faibles, et plus l'albédo solaire est élevé. La même proportion de variation saisonnière a été observée pour les valeurs de LAI. Une équation pour estimer la biomasse des troncs et des branches utilisant des paramètres allométriques et la rétrodiffusion JERS-1 est proposée.
[Traduit par la Rédaction]

Received 11 August 2006. Accepted 17 October 2007. Published on the *Canadian Journal of Remote Sensing* Web site at http://pubs.nrc-cnrc.gc.ca/cjrs on 30 January 2008.

M.D. Bitencourt.[1] Ecology Department, Institute of Biosciences, University of São Paulo (Campus West), Rua do Matão, Trav. 14, No. 321, CEP 05508-90, São Paulo SP, Brazil.

H.N. de Mesquita, Jr. IBAMA, CSR (Remote Sensing Center), Av. L4 Norte, IBAMA Main Building, Block E, CEP 70818-900, Brasília DF, Brazil.

G. Kuntschik. EACH (School of Art, Sciences, and Humanities), University of São Paulo (Campus East), Av. Arlindo Bettio, No. 1000, CEP 03828-000, São Paulo SP, Brazil.

H.R. da Rocha. Atmospheric Sciences Department, Institute of Astronomy, Geophysics and Atmospheric Sciences, University of São Paulo, Rua do Matão, No. 1226, CEP 05508-900, São Paulo SP, Brazil.

P.A. Furley. School of Geosciences, Institute of Geography, University of Edinburgh, Drummond Street, Edinburgh EH8 9XP, UK.

[1]Corresponding author (e-mail: tencourt@ib.usp.br).

Introduction

Phytomass is a vegetation parameter that is crucial in ecology because it is the essential basis of the trophic network and is directly affected by climate change. There are two different aspects regarding phytomass, one related to the amount of leaves and the other to the amount and geometry of trunks and branches. In the case of the *cerrado* biome (the Brazilian savannas), the amount of leaves is related to a gradient of the vegetation structure from open to densely woody physiognomies and is seasonally dependent and strongly related to the radiation balance. The quantity of trunk and branch biomass, however, varies directly with the gradient of vegetation physiognomies. Radar and optical remote sensing provide rapid and nondestructive means of studying or monitoring large-scale biomass vegetation, but their usefulness for the analysis of cerrado vegetation has not been rigorously assessed.

The aim of this paper is twofold: (*i*) assess the value of remote sensing in estimating the structural components of vegetation, and (*ii*) quantify the relationship between the spectral vegetation index and biomass (green leaves, branches, and trunks). To compare the ability of estimating green and aboveground woody biomass using either optical or radar sensors, two case studies were analysed seasonally using two different approaches within two different areas.

Background and context

The cerrado biome (the Brazilian savannas) originally occupied 23% of the Brazilian territory. In 1997, Conservation International suggested that this biome was one of the 18 endangered World Hot Spots. At that time more than 70% of the biome had been cleared for agriculture, especially for soybean production. In the Brazilian state of São Paulo, 14% of the area used to be covered by cerrado, whereas today less than 1% remains preserved, mostly in private hands (Kronka et al., 1993; SMA, 1999). From a Brazilian conservation point of view, study and monitoring of the cerrado has become extremely urgent as a result of the expansion of the agricultural frontier (Silva et al., 2006).

According to Coutinho (1978), the cerrado vegetation comprises a range of physiognomies, from grassland to arboreal formations. The gradient of density, height, and cover of woody species results in different physiognomies with an increasingly woody content from *campo limpo* to *campo sujo*, *campo cerrado*, *cerrado* strictu sensu (s.s.), and *cerradão.* Cerrado latu sensu (l.s.) usually comprises a patchwork of these physiognomies depending on soil, topography, and human impact.

The flora of the cerrado consists of approximately 800 species of trees and a large number of sub-shrubs, shrubs, and herbs and has features typical of pyrophytic savanna vegetation. The trees are of low contorted form with a thick, corky, fire-resistant bark. Sclerophylly is common, and many leaves have thick cuticles, sunken stomata, and greatly lignified and sometimes silicified tissues. Xylopodia are well developed in both the woody and herbaceous vegetation (Furley, 1994; 1999; Ratter and Dargie, 1992; Ratter et al., 1996).

In São Paulo State, the focus of the present study, the cerrado physiognomies vary from campo cerrado to cerrado strictu sensu (s.s.) to cerradão (savanna woodland). Other associated forest types, such as riparian forest and seasonal semideciduous forest (SSForest), can also be found, particularly in the São Paulo portion of the cerrado biome. The cerradão canopy is 10–15 m high and has regular surface height geometry; the SSForest canopy is 15–25 m high and its geometry is relatively rough, mainly because of the presence of emergent trees. The total amount of aboveground woody biomass distinguishes these two vegetation types according to Batalha et al. (2001), who also found that cylindrical volume is the best variable to distinguish the cerrado physiognomies and can be used to estimate the amount of phytomass. The cerrado physiognomies in São Paulo show increasing values of cylindrical volume, from campo cerrado through cerradão (**Table 1**). Mesquita (1998) found a direct relationship between the cylindrical volume and the normalized difference vegetation index (NDVI) obtained from satellite images. With cylindrical volumes varying considerably from the woody and herbaceous components (from campo limpo to cerradão), it is necessary to find the best method to predict the wood and leaf biomass.

The occurrence of dry and wet seasons raises two important questions regarding the vegetation cover in the cerrado biome: What is the best method for estimating green and wood biomass using remote sensing methods? How can optical remote sensing contribute to a better understanding of radiation balance? Green biomass and radiation balance are related to the amount of green leaves present in each physiognomic type and vary seasonally. The more woody physiognomies, however, differ from one another not only in species composition but also in the amount of total aboveground biomass owing to trunks and branches.

Table 1. Cylindrical volume ($m^3 \cdot h^{-1}$) structure descriptors for woody and herbaceous components in three *cerrado* physiognomies.

	Campo cerrado (N = 714)	Cerrado s.s. (N = 399)	Cerradão (N = 301)
Woody component	69.11±29.3	164.79±62.5	428.47±369.2
Herbaceous component	95.98±86.8	38.39±37.2	4.47±7.7

Note: Values in the table are mean cylindrical volumes ± standard deviation for probability $p < 0.001$ (adapted from Batalha et al., 2001). N, number of measurements.

Gower et al. (1999) conducted an extensive analysis of the direct and indirect methods used to estimate the leaf area index (LAI), the fraction of absorbed photosynthetically active radiation (PAR), and net primary production obtained from remotely sensed products. According to Gower et al., all of the available optical instruments are liable to underestimate the LAI, especially when foliage in the canopy is clumped, as it is in the cerrado biome. Gower et al. also compared the LAI obtained from various methods and the vegetation index obtained from satellite images. This experience indicated the potential usefulness of an experiment where simultaneous LAI and NDVI measurements of cerrado physiognomies could be compared with the PAR recorded in the field.

The vegetation index obtained from optical reflectance has been proposed as a good nondestructive method to estimate green biomass or LAI or for classification (Bitencourt-Pereira, 1986; Mesquita, 2003). According to Huete et al. (1999), optical remote sensing is strongly related to the presence of green leaves and can be measured indirectly with the NDVI, which is directly related to LAI and biomass. Huete et al. showed that the NDVI correlates exponentially with the LAI, saturating around LAI = 4. However, the seasonal variation can lead to misinterpretation when optical remotely sensed data are used to measure vegetation cover parameters. Several Brazilian studies have used optical remote sensing to estimate Brazilian cerrado biomass, but the results indicate that such techniques are only applicable for some physiognomies because of the seasonality (Bitencourt et al., 1997; 2004; Mesquita, 1998; Bitencourt, 2004; Mesquita et al., 2005). A number of attempts have been made to estimate campo cerrado green biomass with vegetation indices obtained from multispectral scanner (MSS) Landsat data (Bitencourt-Pereira, 1986; Valeriano and Bitencourt-Pereira, 1988), and some studies have attempted to quantify cerrado s.s. total biomass through vegetation indices obtained from thematic mapper (TM) Landsat data (Santos, 1988).

The L-band microwave signal can penetrate a vegetation canopy and respond to the structure volume. This fact could improve the prospects for vegetation analysis. In recent years microwave images have become useful to ecologists because their signals are more related to aspects of geometry, such as branches and trunks, than to the presence of leaves. The distance between trees can also be measured with L-band microwave. Another advantage is that microwave images are less dependent on weather conditions, allowing images even during the wet season. The potential of synthetic aperture radar (SAR) images like JERS-1 (L band) for the study of cerrado physiognomies has been explored by Santos et al. (1998; 2000; 2002), and the possibility of estimating woody biomass from active remote sensors was explored by Kasischke et al. (1997) and Santos et al. (1998). Imhoff (1995) showed that the correlation between biomass and backscatter is due to the increased scattering volume that occurs from the forest canopy as the aboveground biomass increases. Imhoff contends that the level of saturation in estimating aboveground biomass is limited by the microwave wavelength. He correlated field biomass with C-, L-, and P-band backscattering and found that the C band saturates with less biomass, followed by the L band and the P band. Thus, it is expected that P-band images will be better for estimating biomass because they saturate at a higher biomass. Santos et al. (2003) also explored the use of airborne SAR P band in estimating aboveground biomass in tropical rainforest, opening a new perspective to estimating the biomass of dense physiognomies.

Location and methods

Study areas

The study areas are cerrado remnants taken from a forest inventory of São Paulo State (Kronka et al., 1993). Most of the areas comprise the full range of cerrado physiognomies, as well as some patches of associated vegetation types. **Figure 1** illustrates the location and extent of the cerrado domain in Brazil and São Paulo State.

The first area is a conservation unit (CU), named Gleba Pé-de-Gigante, located in Santa Rita do Passa Quatro Municipality (21°37′S, 47°37′W) and covering approximately 1225 ha (Bitencourt et al., 2004; Mesquita et al., 2004; Bitencourt and Mesquita, 2005). The second area is a set of natural and seminatural vegetation remnants, within private properties, located in Campos Novos Paulista Municipality

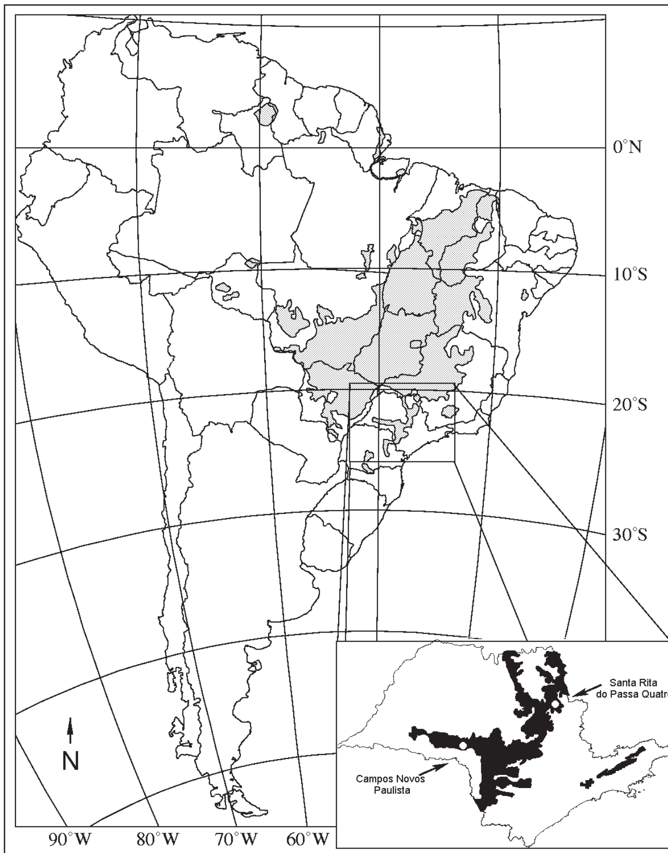

Figure 1. Distribution of the cerrado domain in South America. The inset map shows the extent of cerrado in São Paulo State (IBGE, 1993) and the location of both study areas.

(22°30′S, 50°00′W) and with an area of approximately 1766 ha (Kuntschik and Bitencourt, 2003; Bitencourt et al., 2004).

Both field areas were used to perform two investigations: test the ability of the vegetation index, obtained from optical remote sensing (Landsat and Ikonos), and the LAI, obtained in the field, to be related to radiation balance data obtained in the field; and estimate aboveground woody biomass using radar remotely sensed data (JERS-1). To estimate green leaf density and investigate radiation balance it was necessary to take seasonality into account together with the structure of each cerrado physiognomy. The Pé-de-Gigante CU was found to be appropriate not only because there is a tower collecting daily radiation data, but also because the vegetation cover is well studied and considered to be well preserved. To estimate aboveground woody biomass (AGWB), it was necessary to select appropriate woody cerrado physiognomies with different trees densities. In that case, the conservation stage of the vegetation cover was not considered important.

The Pé-de-Gigante CU was created in 1970, with 1225 ha spread over altitudes ranging from 590 to 740 m. The present vegetation comprises all of the cerrado physiognomic types. Climatically, the region is classified as tropical with wet summers and dry winters, corresponding to Cwa of the Koppen climatic classification. The mean annual precipitation is 1475 mm, and the mean monthly temperature is around 23 °C, with little variation. According to Mesquita (1998), there are 600 ha of cerrado s.s., 404 ha of cerrado s.s. with a thin herbaceous stratum, 49 ha of cerradão, and 114 ha of campo cerrado plus other associated physiognomic types of vegetation. The amount of green leaves in each physiognomic unit was estimated using two methods: reflectance transformed into classes of a vegetation index, and LAI obtained in the field using a nondestructive method. The results were compared with the daily radiation collected (from a tower) during the same period to see whether vegetation indices could be used to estimate radiation balance.

The Campos Novos Paulista is a set of remnants located on private property, for the most part in good conservation condition, which were used collectively to find the relationship between AGWB of cerrado s.s. and cerradão using the regression analysis between the backscattering signal (σ) within L-band SAR images and AGWB obtained from an appropriate allometric biomass equation.

Green leaf estimates and radiation balance

A series of five TM Landsat images was used to obtain the seasonal variation in NDVI (normalized difference vegetation index between near-infrared and red bands). Four images were analysed from 1995 (3 June, 7 July, 22 August, 10 November), and one image was analysed from 1996 (29 January). All images were compensated for atmospheric effects and solar angle and then converted from digital numbers to reflectance (Mesquita, 1998; 2003). **Figure 2** shows the spatial distribution of the physiognomic types in the conservation unit. The polygons defining the area of probable occurrence of the cerrado physiognomies were obtained from the average NDVI, from the dry to wet seasons, for each class. The vegetation structure was measured within an area of 2.7 ha with all physiognomic types. Thus, all trees were measured in 30 permanent plots of 30 m × 30 m, giving data on diameter at ground level, total height, crown height and diameter, species type, and the *X* and *Y* coordinates of the individual tree positions. **Figure 3** illustrates the arrangement of all trees in the sample area with a diameter at ground level greater than 10 cm and the arrangement of the permanent plots. Each circle represents the projection of the circular crown diameter. The plot arrangement shows the physiognomic (crown density) gradient from savanna woodland (cerradão) to the predominantly grassy type of vegetation (campo cerrado).

The pixel size is 30 m for optical Landsat bands and 4 m for Ikonos multispectral bands. Thus, each permanent plot was designed with a maximum size of 30 m × 30 m to be comparable with other satellite images. All permanent plots were arranged in three connected lines, from east to west. This arrangement provides for geographical alignment of both lines of pixels and terrain permanent plots. Because all images are always geocoded with some subpixel uncertainty, the vertices of the terrain polygon were used to obtain the average NDVI value related to each permanent plot.

The LAI estimations were made during the dry and wet seasons (June 2001 and January 2002) using two plant canopy analysers (Li-Cor LAI-2000). In each field trip, 25 records were taken at each permanent plot (a total of 750 records for each period) and used to calculate the mean LAI within each plot. It has been suggested (Gower et al., 1999) that 22 records would be enough to calculate the mean LAI of each plot. The LAI values were compared with the NDVI average of the Ikonos multispectral image from 21 April 2001.

The relationship between vegetation cover and radiation rests on the fact that leaves are responsible for capturing most of the solar energy at the Earth's surface, particularly in the visible PAR band (0.4–0.7 μm). It is expected that the amount of solar energy absorbed by the vegetation cover changes seasonally, especially in biomes like cerrado, which has two prominent seasons (one dry and one wet). Thus, using optical remote sensing data, it is possible to measure the photosynthetically active vegetation and compare it with the amount of energy registered in the field. The spectral vegetation indices, obtained from satellite, are numerical models that have a direct relation with green biomass per area because they result from the spectral responses of the vegetation in the red and near-infrared bands. The spectral response of the vegetation in the red band is due to the presence of chlorophyll, and the spectral response of the vegetation in the near-infrared band is due to leaf structure. Since vegetation indices are proportional to green leaf density and the cerrado physiognomies range from grassland to forest, it is possible to map these physiognomies using vegetation indices.

Mesquita et al. (2004) modeled mean NDVI values, for a hypothetical calendar year, producing curves for all cerrado

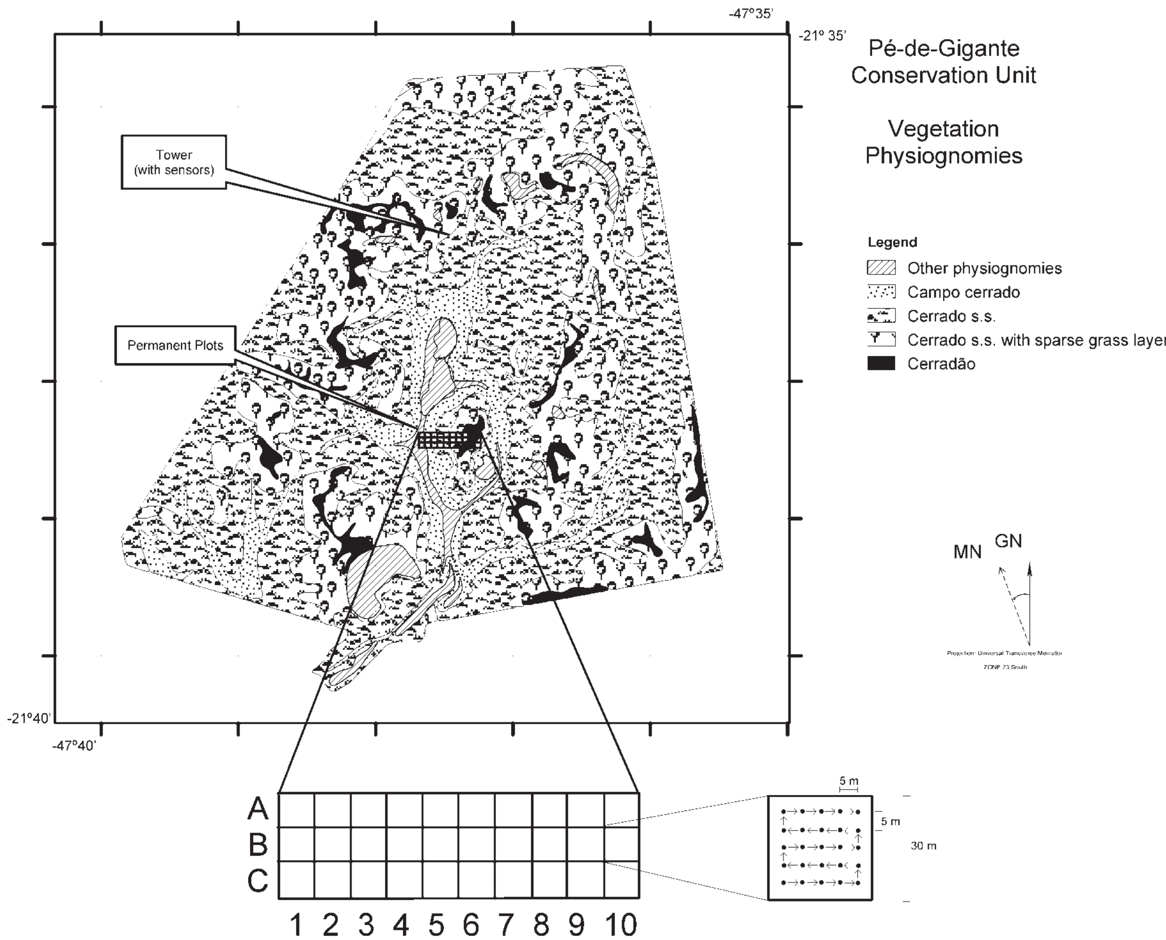

Figure 2. Map of the conservation unit where the green leaf estimates and radiation balance studies took place, the scheme showing the permanent plots where the LAI was estimated, and the field sample arrangement.

physiognomies, using nine Landsat TM images of that CU. The method of analysis, derived from empirical models and meteorological data, showed an encouraging level of results and has considerable potential for improving the understanding of NDVI variation of cerrado vegetation.

LAI can also be used to estimate the total amount of leaves and can vary from 1 to 8, with LAI = 1 corresponding to desert vegetation and LAI = 6 to 8 corresponding to rainforest. Daughtry (1990) reviewed several direct or indirect methods to measure the LAI and the correlation of this information with remote sensing data. His work showed that LAI can be used to estimate the total amount of leaves of each tree of all the vegetation cover. Considering the relationship between LAI and NDVI, we want see if it is possible to correlate solar and PAR albedo, obtained in the field, with NDVI classes obtained with optical remote sensing.

The present study utilized a tower installed in cerrado s.s., with sensors for PAR and solar albedo as illustrated in **Figure 4**. A quantum system (LiCor 190AS sensor) was used to measure the PAR (0.4–0.7 μm) albedo, and a pyranometer was used to measure the total radiation of the solar spectrum (0.28–2.80 μm) with a LiCor 200AS sensor.

Figure 4 shows the plan of the vegetation physiognomy and the tower. The radiation collection period was the whole of 2001. The vegetation classes were abstracted from a map published in Mesquita (1998), and LAI data for each class were collected in the field in June 2001 and January 2002. The NDVI, the vegetation index used in the analysis, is obtained from the reflectance of red and infrared bands from two satellites, namely Landsat TM and Ikonos multispectral. The sphere of detection of the tower sensors is less than 50 m in diameter, covering the cerrado s.s. physiognomy around the tower. Considering that the spatial resolution of Landsat TM is 30 m × 30 m and Ikonos multispectral is 4 m × 4 m, it is acceptable to compare the energy registered in the images and by the tower.

Estimates of aboveground woody biomass

Microwave radiation is emitted from the JERS-1 radar antenna, which also receives the backscattered signal from the Earth's surface. The sigma signal value (σ) is the ratio of the received backscattered energy to the emitted energy. Usually, σ values are expressed in decibels (dB). The pixel values in the original image are in digital numbers (DN). These values can

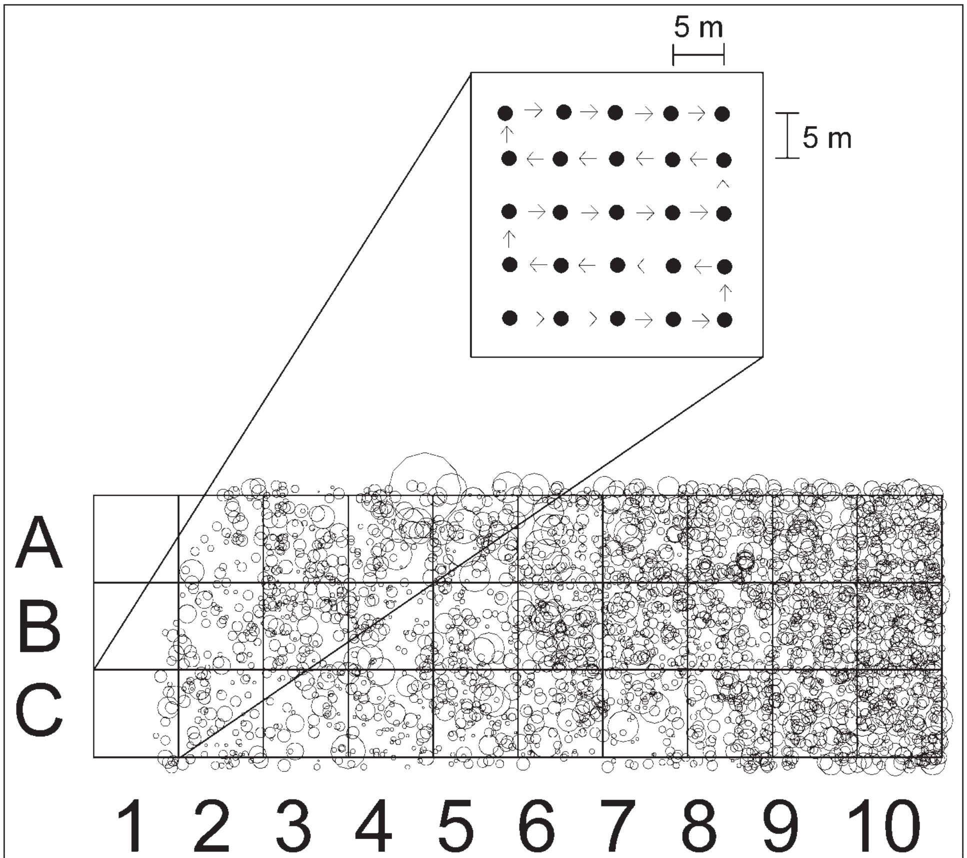

Figure 3. Detail of the field procedure to collect LAI values in 30 permanent plots measuring 30 m × 30 m. Each plot represents the actual vegetation cover identified in the field.

be converted to σ using the following equation (Rosenqvist, 1997; Shimada, 2001):

$$\sigma = 10 \log_{10}\left[\frac{\Sigma(\mathrm{DN}^2)}{n}\right] + \mathrm{CF} \tag{1}$$

where DN is the digital number of a pixel in a 16 bit image, σ is the ratio of received backscattered energy to emitted energy, n is number of pixels sampled, and CF is the calibration factor.

Generally, the σ values are dependent on the geometry of the signal emitted by the antenna and the type of backscatter produced by the target on the ground. The JERS-1 SAR signal interacts with Earth's surface roughness on a magnitude of half of the wavelength (λ = 23 cm) and mostly with objects oriented according to the vertical emission – vertical reception (VV) signal polarization (i.e., tree trunks).

A number of parameters are important in understanding the response of the target on the Earth's surface, including the geometry of the satellite and antenna (satellite ephemeris and antenna angle) in relation to the surface and target (corner reflection and specular reflection). When the satellite is in a descendent orbit (north to south), the antenna views the west side; when the satellite is in an ascendant orbit (south to north), the antenna views the east side. According to the date of the image, it is possible to determine the orbit and antenna angle. This information, together with relief data, can be used to identify the patterns of corner reflection, layover, and shadow in the signal received. Images acquired when the satellite orbit is descendent will have high reflection caused by east hill surfaces over high slope relief (corner effect and incident angle

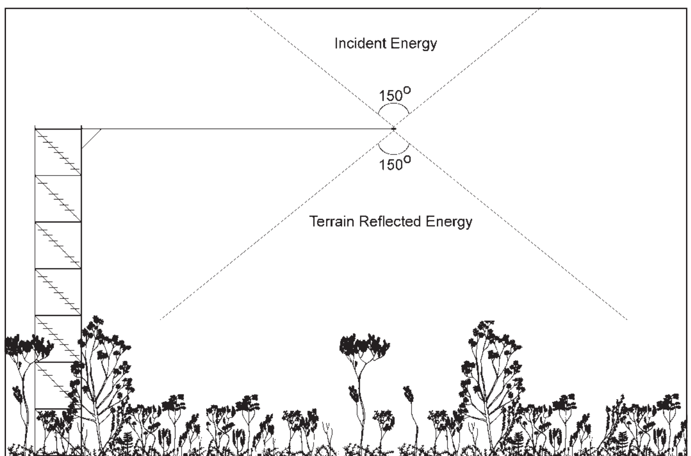

Figure 4. The design of the tower in relation to the vegetation profile.

close to zero), and the opposite applies for an ascendant orbit. According to Luckman et al. (1998), the satellite orbit is important to an understanding of the signal reflected by the target in the JERS-1 SAR images. It is also important to make the conversion using the appropriate factors according to the date of processing of the image. According to the Japan Aerospace Exploitation Agency (JAXA), a factor of –85.34 must be used for images processed after 1 April 2000, which is the case in this study.

SAR L-band images from the JERS-1 satellite were used to calibrate field data with the satellite backscattering response. The SAR L-band image was acquired on 20 December 1995 (path 389, row –338). The data were supplied by the JAXA – University of São Paulo partnership. All digital processing was performed using all or some of the following software: ERDAS Imagine, ERMapper, and ENVI. The fieldwork was undertaken in cerrado remnants located on two farms within the Campos Novos Paulista Municipality. The cerrado remnants are currently surrounded by pasture and, to a lesser degree, cultivation.

An enhanced thematic mapper plus (ETM+) Landsat-7 image (221/076) was also used to select the sample sites within the study area. The optical image was acquired on 26 June 2002 and was geocoded with ground-control points obtained either in the field using a global positioning system (GPS) receiver or from 1 : 50 000 scale topographical maps (IBGE, 1975). A preliminary classification of the vegetation types was performed using the NDVI image. Based on this classification, a rapid floristic survey was conducted in the area (Durigan et al., 2003a; 2003b; Ratter et al., 2000a; 2000b; 2003) to improve the information on vegetation type and conservation conditions. As a result, a structural physiognomic zoning map comprising 10 vegetation classes was constructed to aid the sampling process. In each zone, biophysical data were measured and the results were used to compute the AGWB values. The vegetation was sampled using the point centred quadrant method (Mueller-Dombois and Ellenberg, 1974). Ten sample sites were chosen to analyse the vegetation in the field. Twenty quadrants were randomly spread over each site, and four trees were measured in each quadrant. The parameters measured for each tree include diameter at breast height (DHB), distance from the central tree within each quadrant, and height. The AGWB estimate was made through the application of allometric equations (Equation 2) developed by Abdala et al. (1998):

$$\log(y) = 0.9967\ \log(x) + 2.587 \qquad (2)$$

where y is the total individual weight (g), and x is the cylindrical volume (dm^3). The equation was developed for cerrado s.s and cerradão vegetation types, located in the central portion of the cerrado domain. The AGWB values of these sampled points were related to the σ (backscattering) data recorded in the JERS-1 images.

The SAR L-band image was read, subset, and geocoded to a Universal Transverse Mercator (UTM) projection using the software ENVI. The image was filtered with a 3 × 3 Frost type filter to reduce the effect of speckle noise. **Figure 5** shows the location of the 10 sample sites, inside or outside the cerrado remnants polygons (in grey) obtained from Kronka et al. (1993). The backscattering σ values considered for each sample site are the average values found inside the sample polygons (in black), which are also shown in **Figure 5**.

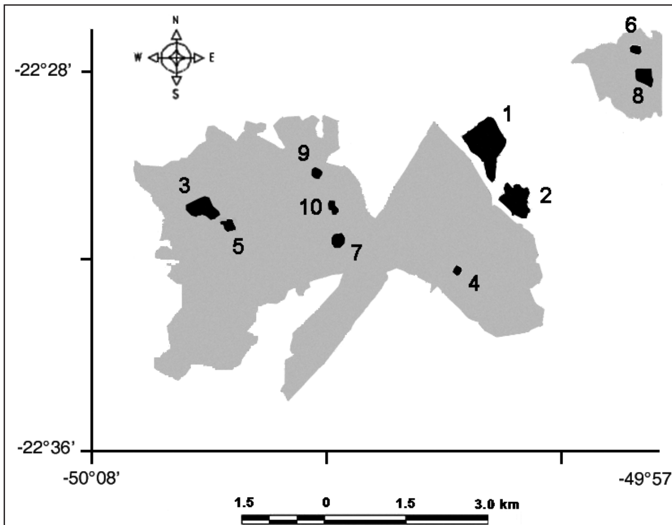

Figure 5. The study area showing the 10 sample sites (in grey polygons) and the sample plot areas (in black polygons) from where the JERS-1 image backscattering and AGWB data were collected.

The sample sites were chosen considering the presence of tree cerrado species, with a wide vegetation cover pattern. Distances between trees and the amount of biomass were considered to be more important than the conservation state of the vegetation cover for the objective of this work because the L-band interaction is expected to be geometrically dependent. To check the geometrical dependency, 10 different sample sites were chosen as follows:

(1) Sample site 1 was an area covered by cerradão, partially deforested for raising cattle. This area is outside the core remnant used in this work (**Figure 5**).

(2) Sample site 2 was an area with a covering similar to that of sample site 1 but with a greater number of remnant large trees. This area is also outside the core remnant used in this work (**Figure 5**).

(3) Sample site 3 was covered by an open type of cerrado s.s. The trees at this site were smaller and more numerous than in the previous sample site.

(4) Sample site 4 was covered by an ecotone that ranged from cerradão to SSForest. There were many trees regrowing from axial buds at the bottoms of trunks. A total of 80 trees were sampled in this area. Among them, 17 showed the phenomenon of multiple axial regrowths. This area was connected with other areas covered by pasture, and it is continuously invaded by cattle, causing harm to the natural regeneration process.

Table 2. LAI values for each permanent plot in both field seasons, June and January, and the predominant physiognomies (in parentheses) based on the plant species found.

	Column									
Row	1	2	3	4	5	6	7	8	9	10
June										
A	0.91 (Cc)	1.25 (Css)	1.09 (Cc)	1.13 (Cc)	1.50 (Css)	2.32 (Css)	2.00 (Cd)	1.88 (Cd)	1.81 (Cd)	1.74 (Cd)
B	1.50 (Css)	1.47 (Css)	1.21 (Cc)	1.17 (Cc)	1.73 (Css)	2.09 (Css)	2.04 (Cd)	2.07 (Cd)	1.52 (Css)	2.18 (Css)
C	1.96 (Css)	1.99 (Css)	1.13 (Cc)	1.43 (Cc)	1.65 (Css)	1.95 (Css)	1.72 (Cd)	2.02 (Cd)	1.73 (Cd)	2.49 (Css)
January										
A	1.09	3.03	2.59	2.73	2.31	2.90	3.07	2.90	2.72	2.78
B	2.00	3.32	2.54	2.55	2.71	3.19	3.38	2.51	2.54	2.63
C	2.33	3.50	2.34	2.43	2.72	2.75	2.90	2.85	2.58	2.68

Note: There were 25 measurements in each plot. Cc, campo cerrado; Cd, cerradão; Css, cerrado s.s.

(5) Sample site 5 was covered by cerradão, with a significant accumulation of litter on the ground surface. This site provided evidence that fires were not frequent in this area, as in many similar areas.

(6) Sample site 6 corresponded to a well-preserved cerradão tract close to the edge of the remnant. The area was clearcut 30 years ago, but since then it has been protected from cattle and thus an advanced regeneration process was evident.

(7) Sample site 7 corresponded to a well-preserved central tract of cerradão with little influence from edge effects.

(8) Sample site 8 had a cerradão vegetation cover and was located to the south of the drainage line.

(9) Sample site 9 was also covered by cerradão and was located alongside the drainage, between sites 8 and 10.

(10) Sample site 10 was covered by cerradão and located in the northern part of the forested drainage strip.

Table 3. Mean LAI value for each cerrado physiognomy in June 2001 and January 2002.

Physiognomy	June 2001	January 2002
Campo cerrado (*N* = 175)	1.15	2.32
Cerrado s.s. (*N* = 350)	1.83	2.76
Cerradão (*N* = 225)	1.89	2.85

Note: Cc, campo cerrado; Cd, cerradão; Cs, cerrado s.s.; *N*, number of measurements in each period.

Results and discussion

Green leaf estimates and radiation balance

The results of the overall LAI mean values, for the dry and wet seasons, are presented in **Table 2**. All plants were identified in each sample plot, providing information on the predominant cerrado subgroups. Thus, in addition to the LAI mean values resulting from 25 records in each plot, there are also data on the predominant physiognomy. The lowest mean LAI values are observed in campo cerrado (A1, A3, A4, B3, B4, C3, and C4, where the letters and numbers denote the row and column, respectively, in **Table 2**), followed by cerrado s.s. (A2, A5, A6, B1, B2, B5, B6, B9, B10, C1, C2, C5, C6, and C10), and cerradão (A7, A8, A9, A10, B7, B8, C7, C8, and C9). **Table 4** illustrates the mean LAI values found for each physiognomic group. Campo cerrado showed a slightly greater variation between seasons, from 1.15 to 2.32, when compared with cerradão, which varied from 1.89 to 2.85. All physiognomies showed LAI values below 4.00, indicating that the NDVI is sufficiently good for prediction (**Tables 3** and **4**).

The relationship between the NDVI obtained from an Ikonos multispectral image and the mean LAI obtained in the field for each permanent plot is shown in **Figure 6**. The LAI data were collected in June 2001. In that year, it was still raining in May and had not dried out by June (**Figure 7**).

The Ikonos image corresponds to the pre-dry period, which should be the best period to discriminate between the cerrado physiognomies using NDVI images obtained with Landsat TM

Table 4. Average NDVI values inside each polygon defined in **Figure 2** corresponding to probable cerrado physiognomies from the dry season to the wet season (from June 1995 to January 1996).

Probable cerrado physiognomy	June 1995	July 1995	August 1995	November 1995	January 1996	Amplitude variation
Campo cerrado	0.49	0.48	0.35	0.6	0.67	0.32
Cerrado s.s.	0.54	0.53	0.41	0.63	0.69	0.28
Cerradão	0.58	0.57	0.48	0.66	0.71	0.22

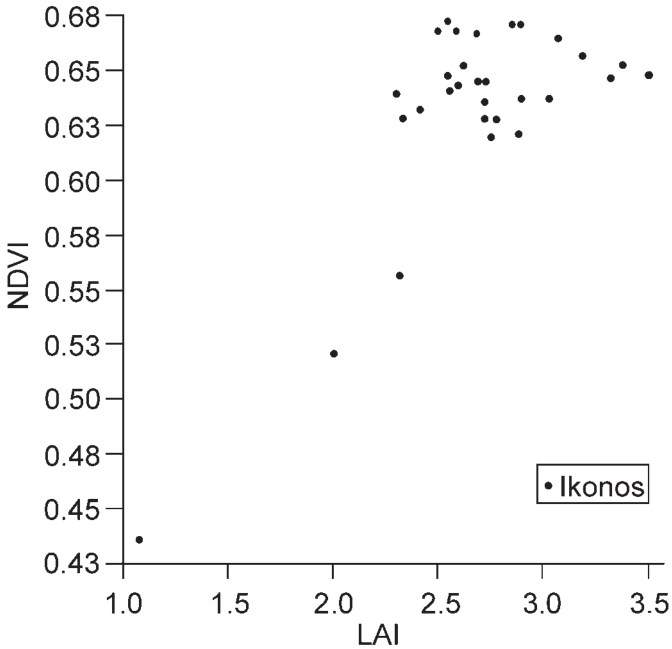

Figure 6. Relationship between NDVI obtained from an Ikonos multispectral image (21 April 2001) and mean LAI estimated in the field for each physiognomic type (June 2001).

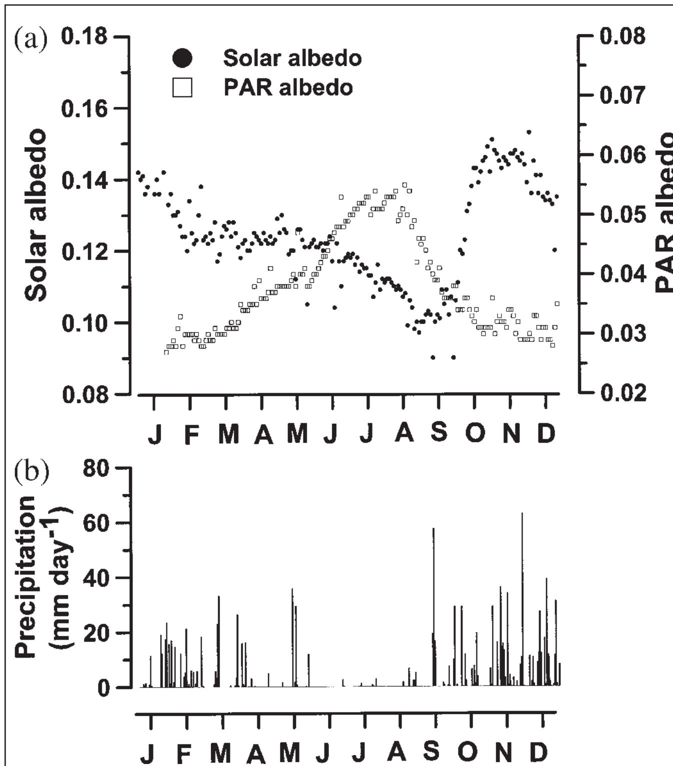

Figure 7. (a) Solar and PAR albedo curves and (b) precipitation data, all collected at the tower during 2001.

(Mesquita, 1998). However, some differences were expected with the Ikonos multispectral NDVI image because the pixel size in that image is 4 m × 4 m as opposed to 30 m × 30 m in the Landsat TM image. The increased spatial resolution of the Ikonos images may also increase reflectance side effects because of exposed soil, litter, and shadow.

The gradient of physiognomic groups shows a significant seasonal variation in NDVI values, from the dry to the wet seasons: campo cerrado from 0.35 to 0.67, cerrado s.s. from 0.41 to 0.69, and cerradão from 0.48 to 0.71 (**Table 3**). Campo cerrado showed an NDVI variation of around 50%, reducing to 30% as the physiognomy changes to cerrado s.s. and cerradão.

Figure 7 shows the solar and PAR albedo data collected from the tower and the precipitation per month during 2001. The inversion observed from July to October reflects the lack of precipitation observed from June to August. PAR albedo increased from 0.028 to 0.052 from February to September (around 50%) and decreased again to 0.028 from October to December because of the reduction in the amount of green leaves that absorbed energy in that portion of the electromagnetic spectrum.

Solar albedo, which includes near-infrared radiation, showed a decrease from 0.08 to 0.17 (>50%) during the dry season. This decrease is also related to the loss of green leaves, which are responsible for high reflectance in the near-infrared region. After September, the regrowth of green leaves increased the measured solar albedo.

The variation in LAI may include dead leaves still held in the vegetation, resulting in some uncertainness. The variation in NDVI is mostly due to the green leaves but may also be affected by the presence of exposed soil, dead biomass, and shadow. Both LAI and NDVI values showed the same trends from the dry to the wet seasons. The vegetation index image is better because it can give a rapid and efficient description of the distribution of green vegetation, with the same level of uncertainty as that offered by the LAI measurements. Thus, the use of NDVI images is as acceptable as the use of LAI, so commonly used to estimate green leaves and, consequently, the radiation balance (Daughtry, 1990; Gower et al., 1999).

The relationship between NDVI and LAI substantiates the hypothesis that the NDVI values increase as LAI values increase, provided the LAI value is below 4.00 (Huete et al., 1999). Further, the NDVI and LAI variations, from campo cerrado to cerradão, observed here showed a pattern similar to that found by Mesquita (2003). In other words, low arboreal cylindrical volume also means low NDVI and low LAI.

The gradient of physiognomies showed a significant seasonal variation in NDVI, with up to a doubling of their values between the dry and wet seasons. The campo cerrado, with lower cylindrical volumes, showed the highest NDVI variation; conversely, the cerradão, with higher cylindrical volumes, showed the lowest NDVI variation. This variation can be associated with the fact that most of the herbaceous stratum suffers as the water supply becomes scarce during the dry season. Perennial trees, on the other hand, can access deeper water supplies and maintain their greenness over a longer period.

The solar and PAR albedo data collected from the tower seem to follow the mean monthly precipitation. The inversion

Table 5. Probable cerrado s.s. radiation balance from the dry season to the wet season.

	Mean NDVI	Precipitation	PAR albedo	Solar albedo
August 1995	0.41	Low		
August 2001	0.34*	Low	High	Low
November 1995	0.63	High		
November 2001	0.70*	High	Low	High

Note: Radiation and precipitation are from **Figure 7**, and the NDVI values with asterisks were simulated using the model of Mesquita et al. (2004).

in albedo curves observed from July and October reflects the lack of precipitation registered from June and August. PAR albedo increased during the dry season from 0.028 to 0.052 (>50%) because of the reduction in the amount of green leaves (low LAI and NDVI) responsible for absorbed energy in that portion of the electromagnetic spectrum.

Solar albedo, which includes near-infrared radiation, showed a decrease from 0.08 to 0.17 (>50%) from the dry to the wet seasons. This decrease is also related to the loss of green leaves, which are responsible for high reflectance in the near-infrared region. After September, new green leaf growth increased the measured solar albedo.

Similar variations were observed in both LAI and NDVI values from the dry to the wet seasons. LAI variation may include standing dead leaves, which may reduce the precision of the measured variation, but NDVI variation is mostly due to the green leaves, although it may also be affected by the presence of exposed soil, standing dead biomass, and shadow. Another advantage of the vegetation index obtained from reflectance images is a rapid and efficient description of the distribution of green vegetation. Thus, the use of NDVI images is as acceptable as the use of the LAI, which is commonly used to estimate green leaves and consequently the radiation balance.

In the study by Mesquita (1998), the yearly variation in NDVI (from the dry to the wet seasons) showed behaviour similar to that of the variation in solar albedo measured by the tower sensors during 2001. This observation suggests an acceptable capability of NDVI images for predicting LAI and radiation balance. The model of Mesquita et al. (2004) was used to simulate NDVI values for cerrado physiognomies. Considering that in 2001 the cerrado s.s. physiognomy remained the same (no burns and no cuts), the following pattern is observed: the lower the NDVI values, the lower the solar albedo and the higher the PAR albedo during August; and the higher the NDVI values, the lower the PAR albedo and the higher the solar albedo during November (**Table 5**).

Aboveground wood biomass estimate

The field data are summarized in **Table 6** as compiled from the analysis of 80 trees observed at each of the 10 samples sites, comprising a total of 800 trees sampled. The backscattering values showed a direct correlation with the AGWB: low σ values indicate low AGWB values, corroborating findings in the literature (Kasischke et al., 1997; Santos et al., 1998). Sample sites 1 and 2 are both outside the core cerrado remnants (Kronka et al., 1993), and the trees found at these sites belong to cerradão physiognomy. The mean cylindrical volume observed at sites 1 and 2 ranges from 664 to 473 dm^3, respectively, and the mean distance between trees ranges from 38.3 and 18.2 m, respectively. The σ values at sites 1 and 2 are lower than those at all other sites. Site 3 comprises cerrado s.s. with trees 11.2 m apart, the AGWB is still low, and σ is slightly lower than that at site 2. Sites 4–10 are cerradão but with different structural conditions because of the differing stages of conservation. Site 4 shows species belonging to the transition between cerradão and SSForest. The mean cylindrical volume is 98.97 dm^3, and the AGWB is five times greater than that at site 3 because the mean distance between trees is three times smaller, with σ similar to that for the cerrado s.s. Sites 5 and 6, containing species typical of cerradão, are quite similar in terms of cylindrical volume, mean distance between trees, and σ mean values lower than that at site 4, with AGWB levels varying from 33.43 to 62.67 $t \cdot ha^{-1}$. Site 5 is badly preserved (BP), and site 6 lies near the edge (NE) of the remnant. Both sites are quite similar in terms of cylindrical volume, AGWB,

Table 6. Sample sites with each predominant physiognomy, mean cylindrical volume, aboveground wood biomass (AGWB), mean distance between trees, and mean backscattering value (σ).

Sample site	Predominant physiognomy	Mean cylindrical volume (dm^3)	AGWB ($t \cdot ha^{-1}$)[a]	Mean distance (m)	Mean σ (dB)
1	Cerradão trees	664.18	3.32	38.29	–14.53
2	Cerradão trees	472.81	4.89	18.82	–10.99
3	Cerrado s.s.	226.74	6.60	11.20	–9.79
4	Cerradão–SSForest	98.97	32.24	3.30	–9.03
5	Cerradão BP	167.29	55.80	3.30	–8.93
6	Cerradão NE	138.02	60.53	3.20	–8.49
7	Cerradão FE	240.45	90.08	2.20	–7.90
8	Cerradão	168.02	69.89	3.55	–7.04
9	Cerradão AD	290.75	108.27	3.13	–7.48
10	Cerradão AD	335.12	120.35	3.55	–7.18

[a]Estimated using the equation of Abdala et al. (1998)

distance between trees, and σ values. Site 7, which is far from the edge (FE), has a higher cylindrical volume, AGWB, distance between trees, and σ values compared with those of the previous sites. According to IBGE (1975), site 7 was a pasture more than 25 years before our study was conducted. The only exception is a strip located alongside a drainage channel that runs approximately north to south. In this area, the only portion that appeared to be covered by forest-like vegetation 25 years ago is currently covered by cerradão, with some evidence of past fire (charcoal-covered cork found in some individuals). For that reason, three sites were sampled to the north, centre, and south. Site 8 is a denser form of cerradão (cylindrical volume 167.29 dm^3 and distance between trees of 2.23 m), showing higher AGWB and σ mean values. Lastly, sites 9 and 10, which are located along the drainage (AD) line, give the highest AGWB, corroborated by the cylindrical volume, with σ mean values among the highest values. The cylindrical volume values (due to the woody portion only) were used to calculate AGWB but can also be associated with the conservation status: sites 1 and 2 were managed to maintain only the largest trees. The σ mean values are directly proportional to AGWB to around 130 $t \cdot ha^{-1}$ and inversely proportional to the distance between trees (the sparser the trees, the smaller the SAR L-band backscattering).

Figure 8 shows an asymptotic curve relating AGWB, obtained from field data, using an allometric equation, with σ mean values obtained from the SAR L-band image. The AGWB values from less dense physiognomies correspond to the lowest σ values, and those from denser physiognomies correspond to the highest σ values.

The following equation derived from the regression analyses shows a very good coefficient of determination ($R^2 = 0.8714$), making it useful for estimating AGWB in other cerrado areas:

$$Y = 1.5135 \ln(\text{dB or } \sigma) - 14.924 \quad (3)$$

The results suggest a stable tendency but up to 70 $t \cdot ha^{-1}$ of biomass, where the backscattering values start to increase at a lower rate. The increasing AGWB values at sites 6–10 do not have the same backscattering variation as at sites 1–5. The behaviour of the curve supports the usefulness of the L-band radar images, specifically those of the JERS-1 microwave sensor, for estimating forest AGWB up to a threshold value of 100 $t \cdot ha^{-1}$ in areas covered by cerrado s.s. and cerradão. The microwaves interact with tree trunks and branches, and the returned signal is related to the amount of AGWB. However, the signal is influenced by both living and dead trees. It is therefore necessary to take the total AGWB into account.

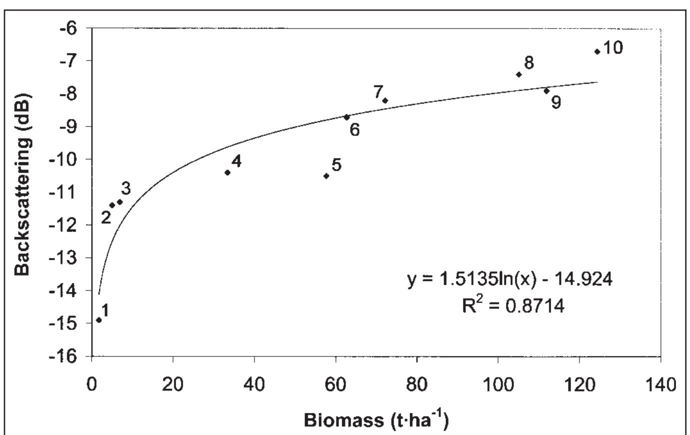

Figure 8. Curve showing the relationship between the forest aboveground woody biomass (AGWB) values and the backscattering (σ) values in the JERS-1 image.

Santos et al. (2002) also used JERS-1 images to quantify AGWB in the contact zone between rainforest and cerrado in the Brazilian states of Roraima and Mato Grosso. Although that study showed higher AGWB values, the shape of the curve was similar to that in the present study, suggesting that if SAR data can estimate rainforest biomass, they can also estimate cerrado l.s. vegetation because it is less dense than a rainforest.

The validity of the present work may be jeopardized by the fact that the SAR L-band image was acquired by the JERS-1 satellite 6 years before the fieldwork was undertaken, and changes in the vegetation are likely to have occurred during this period of time. However, during the vegetation survey under the BIOTA/FAPESP project from 1999 to 2003, the vegetation inside the remnants was considered to be very well preserved, which supports the results from this study. Thus, the results suggest that L-band radar imagery is suitable for AGWB quantification in cerrado areas.

Conclusions

The multiwavelength approach used in this paper allows the characterization of vegetation by indirect measurements. The results obtained with the normalized difference vegetation index (NDVI) series of Landsat images provide a comprehensive understanding of vegetation structure. This approach allows us to infer the vegetation dynamic processes detected from the tower, allowing an extrapolation to the entire conservation unit. The tower results provide very high temporal resolution information about the vegetation dynamics throughout the year that can be related to seasonal variation. The variation in the amount of green leaves in the cerrado gradient of vegetation physiognomies can be rapidly and efficiently estimated using a spectral vegetation index obtained from optical remote sensing (NDVI). The radiation balance, in each vegetation type, can be measured daily using field sensors located in towers. However, because of the high cost of having a tower in each separate physiognomic type, the use of NDVI images is the best way to estimate the radiation balance seasonally because the NDVI values showed the same tendency.

The measurements of solar albedo also correlated with other physical environment parameters that can be used as a component of high-order environmental models. The radiation balance from the dry season to the wet season, measured in the field, varied in the same proportion as the LAI and NDVI changes, obtained respectively from the plant canopy analyser and from NDVI images. The spectral response of the green leaves closely matched the results from remotely sensed data, a feature that has not been reported in the literature so far. NDVI values are directly related to LAI (where LAI < 4) and PAR, which can be used to estimate net primary production. Because the NDVI is only related to green leaves, however, a different method is needed to estimate branch and trunk biomass.

The aboveground woody biomass (AGWB) showed a very good coefficient of determination (R^2 = 0.8714) with the data from the JERS-1 image. The estimation equation (i.e., Equation 2) found here, which uses allometric parameters of 800 trees, provides a reliable nondestructive technique for predicting aboveground biomass in areas with similar vegetation density. SAR L-band data showed better results than optical vegetation index images for both cerradão and cerrado s.s. The radar images can be used to map the spatial distribution of different classes of cerrado vegetation and to estimate the amount of carbon in the biomass. There is still discussion about the upper limit of biomass that can be detected from L-band SAR images, which may lie somewhere between 100 and 120 $t \cdot ha^{-1}$. The ecological importance of phytomass estimation makes it essential to look for new nondestructive methods. The JERS-1 images are especially helpful because the microwaves are independent of weather conditions (transparent to clouds and rain). In the near future, other SAR bands will become available, such as P band, which is expected to estimate phytomass with greater precision. Also in the future, there is the option of band polarization, which will further improve the nondestructive estimation of phytomass. Another important point is the geometric relationship between SAR L band and the distance between trees: the sparser the trees, the lower are σ values. This observation cannot be made if all sample sites have the same conservation pattern. The availability of polarimetric sensors, such as the Japanese phased array L-band synthetic aperture radar (PALSAR) on the Advanced Land Observation Satellite (ALOS), would increase the capability of AGWB estimation through remote sensing.

Acknowledgements

The authors wish to express their gratitude to the University of São Paulo and the Japan Aerospace Exploitation Agency (JAXA) for providing the image used. We wish to thank the Fundação de Amparo à Pesquisa do Estado de São Paulo (FAPESP) for financial support and scholarships in the BIOTA/FAPESP Programme (Biodiversity Virtual Institute Program, www.biota.org.br.).

References

Abdala, G.C., Caldas, L.S., Haridasan, M., and Eiten, G. 1998. Above and below ground organic matter and root:shoot ratio in a cerrado in central Brazil. *Brazilian Journal of Ecology*, Vol. 2, pp. 11–23.

Batalha, M.A., Mantovani, W., and de Mesquita, Jr., H.N. 2001. Vegetation structure in cerrado physiognomies in southeastern Brazil. *Brazilian Journal of Biology*, Vol. 61, pp. 475–483.

Bitencourt, M.D. 2004. Diagnóstico cartográfico dos remanescentes de cerrado em São Paulo. In *Viabilidade de conservação dos remanescentes de cerrado do estado de São Paulo*. Edited by M.D. Bitencourt and R.R. Mendonça. Annablume, São Paulo, Brazil. pp. 17–28.

Bitencourt, M.D., and Mesquita, Jr., H.N. 2005. Análise ambiental espacializada. In *Cerrado Pé-de-Gigante: ecologia e conservação – Parque Estadual de Vassununga – São Paulo*. Edited by Vânia Regina Pivello and Elenice Mouro Varanda. SMA Press, São Paulo, Brazil. Chapter 3, pp. 43–50.

Bitencourt, M.D., Mesquita, Jr., H.N., Mantovani, W., Batalha, M.A., and Pivello, V.R. 1997. Identificação de fisionomias de cerrado com imagens índice de vegetação. In *Contribuição ao conhecimento ecológico do Cerrado*. Edited by L. Leite and C.H. Saito. University of Brasília, Brasília, Brazil. pp. 316–320.

Bitencourt, M.D., Mesquita, Jr., H.N., and Kuntschik, G. 2004. Describing savannas physiognomies and seasonal tropical forests using temporal SAR (JERS-1) and optical images (Landsat) in São Paulo State, Brazil. In *JERS-1 Research Invitation Program — Final Report*. EORC/JAXA, Tokyo. Vol. 1, pp. 53–73.

Bitencourt-Pereira, M.D. 1986. *Correlação de fitomassa foliar de campo cerrado com dados espectrais obtidos pelo sistema MSS-Landsat e por radiometria de campo*. São José dos Campos, Brazil. Boletin do INPE-3747-TDI-203.

Coutinho, L.M. 1978. O conceito de cerrado. *Revista Brasileira de Botânica*, Vol. 1, pp. 17–23.

Daughtry, C.S.T. 1990. Direct measurements of canopy structure. *Remote Sensing Reviews*, Vol. 5, pp. 13–26.

Durigan, G., Siqueira, M.F., Franco, G.A.D.C., Bridgewater, S., and Ratter, J.A. 2003a. The vegetation of priority areas for cerrado conservation in São Paulo State, Brazil. *Edinburgh Journal of Botany*, Vol. 60, pp. 217–241.

Durigan, G., Ratter, J.A., Bridgewater, S., Siqueira, M.F., and Franco, G.A.D.C. 2003b. Padrões fitogeográficos do cerrado paulista sob uma perspectiva regional. *Hoehnea*, Vol. 30, pp. 39–51.

Furley, P.A. 1994. Savanna formations: ecology and environment. *Progress in Physical Geography*, Vol. 18, pp. 276–294.

Furley, P.A. 1999. The nature and diversity of neotropical savanna vegetation with particular reference to the Brazilian cerrados. *Global Ecology and Biogeography*, Vol. 8, pp. 223–241.

Gower, S.T., Kucharik, C.J., and Norman, J.M. 1999. Direct and indirect estimation of leaf area index, fAPAR, and net primary production of terrestrial ecosystems. *Remote Sensing of Environment*, Vol. 70, pp. 29–51.

Huete, A., Justice, C., and Van Leeuwen, J.D. 1999. *MODIS vegetation index (Mod 13) algorithm theoretical basis document version 3*. University of Arizona, Tucson, Ariz.

IBGE. 1975. *Mapa topográfico de Campos Novos Paulista SF-22-Z-A-V-2*. Scale 1 : 50.000. Instituto Brasileiro de Geografia e Estatística (IGBE), Rio de Janeiro.

IBGE. 1993. *Mapa da Vegetação do Brasil*. Scale 1 : 5 000 000. Instituto Brasileiro de Geografia e Estatística (IGBE), Rio de Janeiro.

Imhoff, M. 1995. Radar backscatter and biomass saturation: ramifications for global biomass inventory. *IEEE Transactions on Geoscience and Remote Sensing*, Vol. 33, pp. 511–518.

Kasischke, E., Melack, J.M., and Dobson, M.C. 1997. The use of image radars for ecological applications – A Review. *Remote Sensing of the Environment*, Vol. 59, pp. 141–156.

Kronka, F., Matsukuma, C.K., Nalon, M.A., Del Cali, I.H., Rossi, M., Mattos, I.F.A., Shin-Ike-Ywane, M.S., and Pontinhas, A.A.S. 1993. *Inventário florestal do Estado de São Paulo.* Instituto Florestal do Estado de São Paulo/SMA, São Paulo, Brazil.

Kuntschik, G., and Bitencourt, M.D. 2003. Quantificação de fitomassa florestal aérea de cerrado e cerradão através de imagens orbitais SAR. In *Proceedings of the 11th Brazilian Symposium on Remote Sensing*, 5–11 April 2003, Belo Horizonte. INPE, Belo Horizonte, MG Brazil. pp. 2201–2208.

Luckman, A., Baker, J.R., Honzák, M., and Lucas, R. 1998. Tropical forest biomass density estimation using JERS-1 SAR: seasonal variation, confidence limits and application to image mosaics. *Remote Sensing of Environment*, Vol. 63, pp. 126–139.

Mesquita, Jr, H.N. 1998. *Análise temporal com sensor orbital de unidades fisionômicas de cerrado na Gleba Pé-de-Gigante (Parque Estadual de Vassununga – SP).* Masters dissertation, Biosciences Institute, University of São Paulo, São Paulo, Brazil. Available from www.teses.usp.br/teses/disponiveis/41/41134/tde-27072001–092749/.

Mesquita, Jr., H.N. 2003. *Modelagem das variações da resposta espectral das fisionomias de cerrado em relação às variações climáticas sazonais*. Doctoral thesis, Biosciences Institute, University of São Paulo, São Paulo, Brazil. 244 pp.

Mesquita, Jr., H.N., Malthus, T.J., Bitencourt, M.D., and Furley, P.A. 2004. Structural–functional model to remote sensing of vegetation physiognomies seasonal variation based on life form. In *Proceedings of the 4th International Workshop on Functional–Structural Plant Models*, 7–11 June 2004, Montpellier, France. Edited by C.H. Godin, J. Kurth, W. Lacointe, A. Takenaka, A. Prusinkiewicz, P. DeJong, T.M. Beveridge, and C.B. Andrieu. UMR AMAP, Montpellier, France. Vol. 1, pp. 339–343.

Mesquita, Jr., H.N., Bitencourt, M.D., and Rocha, H.R. 2005. Sazonalidade da vegetação e Balanço de radiação. In *Cerrado Pé-de-Gigante: ecologia e conservação – Parque Estadual de Vassununga — São Paulo: São Paulo*. Edited by V.R. Pivello and E.M. Varanda. SMA, Capítulo 12, Brazil. pp. 163–172.

Mueller-Dombois, D., and Ellenberg, H. 1974. *Aims and methods of vegetation ecology.* Wiley, New York.

Ratter, J.A., and Dargie, T.C.D. 1992. Analysis of the floristic composition of 26 cerrado areas in Brazil. *Edinburgh Journal of Botany*, Vol. 49, pp. 235–250.

Ratter, J.A., Bridgewater, S., Atkinson, R., and Ribeiro, J.F. 1996. Analysis of the floristic composition of the Brazilian Cerrado vegetation II: comparison of the woody vegetation of 98 areas. *Edinburgh Journal of Botany*, Vol. 53, pp. 153–180.

Ratter, J.A., Ribeiro, J.F., and Bridgewater, S. 2000a. Woody flora distribution of the Cerrado Biome: phytogeography and conservation priorities. In *Tópicos atuais em botânica*. Edited by T.B. Cavalcanti and B.M.T. Walter. Recursos Genéticos e Biotecnologia & Sociedade Botânica do Brazil, EMBRAPA, Brasília. pp. 340–342.

Ratter, J.A., Bridgewater, S., Ribeiro, J.F., Dias, T.A.B., and Silva, M.R. 2000b. *Distribuição das espécies lenhosas da fitofisionomia Cerrado sentido restrito nos estados compreendidos pelo bioma Cerrado*. Boletim do Herbário Ezechias Paulo Heringer 5, pp. 5–43.

Ratter, J.A., Bridgewater, S., and Ribeiro, J.F. 2003. Analysis of the floristic composition of the Brazilian cerrado vegetation III: Comparison of woody vegetation of 380 areas. *Edinburgh Journal of Botany*, Vol. 60, pp. 59–109.

Rosenqvist, A. 1997. *Analysis of the backscatter characteristic of rubber, oil palm and irrigated rice in multiband polarimetric synthetic aperture radar imagery*. Ph.D. thesis, Institute of Industrial Science, University of Tokyo, Tokyo.

Santos, J.R. 1988. *Biomassa aérea da vegetaçao de cerrado: estimativa e correlação com dados do sensor TM-Landsat.* Ph.D. thesis, Federal University of Paraná, Curitiba, Brazil. 208 pp.

Santos, J.R., Xaud, M.R., and Lacruz, M.S.P. 1998. Analysis of backscattering signals of JERS-1 image from savanna and tropical rainforest biomass in Brazilian Amazônia. *International Archives of Photogrammetry and Remote Sensing*, Vol. 32, pp. 523–526.

Santos, J.R., Keil, M., Araújo, L.S., Pardi Lacruz, M.S., Krämer, J.C.M., and Kandler, O. 2000 Biomass estimation of forest and savanna transition vegetation zone by JERS-1 and SIR-C backscatter data. *International Archives of Photogrammetry and Remote Sensing*, Vol. 33, pp. 377–381.

Santos, J.R., Pardi Lacruz, M.S., Araujo, L.S., and Keil, M. 2002. Savanna and tropical rainforest biomass estimation and spatialization using JERS-1 data. *International Journal of Remote Sensing*, Vol. 23, pp. 1217–1229.

Santos, J.R., Freitas, C.C., Araujo, L.S., Dutra, L.V., Mura, J.C., Gama, F.F., Soler, L.S., and Sant'Anna, S.J.S. 2003. Airborne P-band SAR applied to the aboveground biomass studies in the Brazilian tropical rainforest. *Remote Sensing of Environment*, Vol. 87, pp. 482–493.

Shimada, M. 2001. *User's guide to NASDA's SAR products*. Version 2. National Space Development Agency of Japan (NASDA), Tokyo, Japan.

Silva, J.F., Fariñas, M.R., Felfili, J.M., and Klink, C.A. 2006. Spatial heterogeneity, land use and conservation in the cerrado region of Brazil. *Journal of Biogeography*, Vol. 33, No. 3, pp. 536–548.

SMA. 1999. *Conhecer para conservar: as unidades de conservação do Estado de São Paulo.* Terra Virgem, SMA, São Paulo, Brazil.

Valeriano, D.M., and Bitencourt-Pereira, M.D. 1988. Relationships between spectral reflectance and phytomass of the ground layer community of neotropical savanna (cerrado). *International Archives of Photogrammetry and Remote Sensing, Commission VII*, Vol. 27, Part B10, pp. 649–657.